RESEARCH ARTICLE

CceR and AkgR Regulate Central Carbon and Energy Metabolism in Alphaproteobacteria

Saheed Imam,[a,b,c] Daniel R. Noguera,[c,d] Timothy J. Donohue[b,c]

Graduate Program in Cellular and Molecular Biology,[a] Department of Bacteriology,[b] DOE Great Lakes Bioenergy Research Center,[c] and Department of Civil and Environmental Engineering,[d] University of Wisconsin Madison, Madison, Wisconsin, USA

ABSTRACT **Many pathways of carbon and energy metabolism are conserved across the phylogeny, but the networks that regulate their expression or activity often vary considerably among organisms. In this work, we show that two previously uncharacterized transcription factors (TFs) are direct regulators of genes encoding enzymes of central carbon and energy metabolism in the alphaproteobacterium *Rhodobacter sphaeroides*. The LacI family member CceR (RSP_1663) directly represses genes encoding enzymes in the Entner-Doudoroff pathway, while activating those encoding the F_1F_0 ATPase and enzymes of the tricarboxylic acid (TCA) cycle and gluconeogenesis, providing a direct transcriptional network connection between carbon and energy metabolism. We identified bases that are important for CceR DNA binding and showed that DNA binding by this TF is inhibited by 6-phosphogluconate. We also showed that the GntR family TF AkgR (RSP_0981) directly activates genes encoding several TCA cycle enzymes, and we identified conditions where its activity is increased. The properties of single and double ΔCceR and ΔAkgR mutants illustrate that these 2 TFs cooperatively regulate carbon and energy metabolism. Comparative genomic analysis indicates that CceR and AkgR orthologs are found in other alphaproteobacteria, where they are predicted to have a conserved function in regulating central carbon metabolism. Our characterization of CceR and AkgR has provided important new insight into the networks that control central carbon and energy metabolism in alphaproteobacteria that can be exploited to modify or engineer new traits in these widespread and versatile bacteria.**

IMPORTANCE **To extract and conserve energy from nutrients, cells coordinate a set of metabolic pathways into integrated networks. Many pathways that conserve energy or interconvert metabolites are conserved across cells, but the networks regulating these processes are often highly variable. In this study, we characterize two previously unknown transcriptional regulators of carbon and energy metabolism that are conserved in alphaproteobacteria, a group of abundant, environmentally and biotechnologically important organisms. We identify the genes they regulate, the DNA sequences they recognize, the metabolite that controls the activity of one of the regulators, and conditions where they are required for growth. We provide important new insight into conserved cellular networks that can also be used to improve a variety of hosts for converting feedstock into valuable products.**

Received 21 December 2014 **Accepted** 29 December 2014 **Published** 3 February 2015

Citation Imam S, Noguera DR, Donohue TJ. 2015. CceR and AkgR regulate central carbon and energy metabolism in alphaproteobacteria. mBio 6(1):e02461-14. doi:10.1128/mBio.02461-14.

Editor Louis M. Weiss, Albert Einstein College of Medicine

Address correspondence to Timothy J. Donohue, tdonohue@bact.wisc.edu.

This article is a direct contribution from a Fellow of the American Academy of Microbiology.

To survive in nature, cells must metabolize and conserve energy within available nutrients. Cells often use transcriptional networks to sense nutrient availability and orchestrate changes in the activities of metabolic pathways that are needed to acquire energy from available nutrients (1, 2). We are interested in understanding the transcriptional networks that control bacterial carbon and energy metabolism because of the important roles that these pathways play in the physiology of free-living organisms, in microbial communities, or in improving biological hosts for agricultural, health, or industrial use.

Changes in carbon source availability have major impacts on cell metabolism and energetics. Analysis of the transcriptional regulatory networks (TRNs) that regulate carbon and energy metabolism has identified different control strategies in individual species. In *Escherichia coli*, the cyclic AMP (cAMP) receptor protein (Crp) allows the preferential utilization of glucose over other carbon sources (3). In addition, the *E. coli* ArcAB two-component system represses large portions of its central metabolic pathways, including genes encoding tricarboxylic acid (TCA) cycle and respiratory enzymes (4, 5). The LacI family transcription factor (TF) Cra/FruR also regulates carbon and energy metabolism in *E. coli* and related enteric bacteria (6–8). In *Bacillus subtilis*, CcpA mediates glucose catabolite repression by activating expression of glycolytic enzymes while repressing genes encoding proteins needed to metabolize other carbon sources (9, 10). In some beta- and gammaproteobacteria, use of the Entner-Doudoroff (ED) pathway as a route for carbon metabolism is transcriptionally controlled by the RpiR family TF HexR (11–13).

This paper reports on TFs that control central carbon and energy metabolism in the alphaproteobacterium *Rhodobacter sphaeroides*. Alphaproteobacteria are a diverse group of bacteria that include free-living species, as well as species that can enter into beneficial or pathogenic relationships with plants and animals (14, 15). Many alphaproteobacteria carry out important metabolic activities not found in other well-studied systems (e.g., photosynthesis, carbon dioxide, nitrogen fixation, etc.), while others have potential industrial use for the production of fuels or specialty chemicals (14–20).

R. sphaeroides is one of the best-studied alphaproteobacteria from biochemical, genetic, and genomic perspectives (17, 21). This facultative bacterium can grow by aerobic respiration, anaerobic respiration (using alternative electron acceptors, such as dimethyl sulfoxide), or anoxygenic photosynthesis (17, 21, 22). As a result, *R. sphaeroides* has been used as a model system to study the process and transcriptional control of carbon fixation and photosynthesis (23–27). In addition, *R. sphaeroides* can utilize a wide array of nutrients for growth, including at least 68 different carbon sources (28). Studies of carbon flow during growth on glucose and/or gluconeogenic substrates using metabolic flux (29), flux balance, and mutational analyses (22, 28) revealed the important contribution of the ED pathway to central carbon metabolism. However, despite the metabolic diversity of this and other alphaproteobacteria, the TRNs that control central carbon metabolism have not been studied in detail in these bacteria. The *R. sphaeroides* TRN is predicted to contain several gene clusters that are enriched for functions involved in central carbon and energy metabolism (30). Two of these clusters were predicted to be regulated by the previously uncharacterized TFs, RSP_1663 (a LacI family TF here referred to as central carbon and energy metabolism regulator [CceR]) and RSP_0981 (a GntR family TF here referred to as alpha-ketoglutarate regulator [AkgR]) (30).

In this work, we show that CceR is required for normal growth on many carbon sources and that it directly regulates transcription of genes encoding ED pathway and TCA cycle enzymes, the F_1F_0 ATPase, and others. We experimentally verified the predicted DNA sequence motif recognized by CceR and showed that the ED pathway intermediate, 6-phosphogluconate, controlled DNA binding by this TF. We also show that AkgR directly regulates transcription of genes encoding several TCA cycle enzymes and that this TF is important for normal growth when using carbon sources that require high flux through these reactions. Our data provide important new insights into previously uncharacterized TFs that control carbon and energy metabolism in *R. sphaeroides* and likely other alphaproteobacteria containing orthologs of CceR and AkgR.

RESULTS

CceR is a regulator of central carbon and energy metabolism in *R. sphaeroides*. If CceR regulates central carbon and energy metabolism in *R. sphaeroides*, a *cceR* deletion strain might be expected to exhibit growth defects with one or more carbon sources. To test this hypothesis, we constructed and analyzed the growth of a strain containing an in-frame markerless deletion of *cceR* (the ΔCceR strain). Under aerobic conditions in Sistrom's minimal medium (SMM) (31) containing succinate as the main carbon source, the ΔCceR strain grew about 1.5 times slower than its wild-type (WT) counterpart (Fig. 1A). Under photosynthetic (anaerobic in the presence of light) conditions, the ΔCceR strain had a doubling time at least 3 times slower than WT cells on succinate-based SMM (Fig. 1B). Control experiments showed that expressing *cceR* from an inducible low-copy-number plasmid restored the growth rate of the ΔCceR mutant in succinate-containing SMM to that of WT cells (Fig. 1A and B). Thus, we conclude that CceR has an important role, particularly under anaerobic photosynthetic conditions, when using succinate as the major carbon source.

When we compared aerobic growth of the ΔCceR mutant to WT cells in medium containing one of 25 different carbon sources, we observed significantly slower growth of the mutant on 15 of these compounds (Fig. 1C). The severest defect in aerobic growth of the ΔCceR mutant was observed when using carboxylic and amino acids, with up to a 6-fold difference in growth rate between ΔCceR and WT cells when using pyruvate as a carbon source. The only carboxylic acids that permitted normal growth of the ΔCceR strain were acetate and L-tartrate (Fig. 1C). On the other hand, the growth rates of ΔCceR and WT cells were generally similar on all the sugars we tested as carbon sources (Fig. 1C). These data indicate that CceR is needed for normal growth on many carbon sources.

CceR regulates the expression of many metabolic pathways. To gain further insight into the role of CceR, we used global gene expression analyses to identify genes directly or indirectly regulated by this TF. We found that RNA levels from 225 genes were differentially expressed between the WT and ΔCceR cells (cutoff of 1.5 fold change [FC], $P < 0.01$) (see Dataset S1 in the supplemental material) during aerobic growth on succinate-based SMM, with transcripts from 125 genes present at higher levels and transcripts from 100 genes decreased in WT cells relative to the mutant. Some 54 of these differentially expressed genes are annotated as having a role in carbon source uptake or utilization, electron transport, and energy metabolism. Among 31 of the differentially expressed genes that are predicted to encode proteins involved in central carbon and energy metabolism (Fig. 2A) were those encoding enzymes of the ED pathway (*zwf*, *pgl*, and *eda*), the TCA cycle (*sdhDA*, *mdh*, *fumC*, *sucCD*, and *sucB*), glycolysis/gluconeogenesis (*pgi*, *fbaB*, fructose 1,6-bisphosphatase, malic enzyme, *pdhAB*, and *pckA*), and bioenergetic enzymes or electron carriers (*atpBEF*, *atpHAC*, *nuoL*, and cytochrome c_{554}) (Fig. 2A). RNA levels of most of these genes were higher in the WT strain than in ΔCceR cells, suggesting they are activated by CceR. Conversely, RNA levels from genes encoding the ED pathway enzymes (*zwf*, *pgl*, and *eda*) and RSP_2785 (cytochrome c_{554}) were less abundant in WT cells, suggesting they are repressed by CceR (Fig. 2A). Combined, these data predict that CceR is both a positive and negative regulator of gene expression.

Most of the other genes that were differentially expressed in a CceR-dependent manner encoded functions either relating to protein synthesis or biosynthesis of pigments in the *R. sphaeroides* photosynthetic apparatus (see Dataset S1 in the supplemental material). Consistent with these data, we observed increased pigmentation of the ΔCceR strain in the presence of O_2 that was alleviated in the complemented strain, indicating that this trait was also due to loss of CceR function. The increased expression of photopigment-related genes in the absence of CceR may reflect an altered oxidation reduction state of the cell. For instance, the observed differential expression of genes encoding electron transport proteins in ΔCceR cells (see above and Fig. 2A; see also Dataset S1) could alter activity of the PrrAB two-component system,

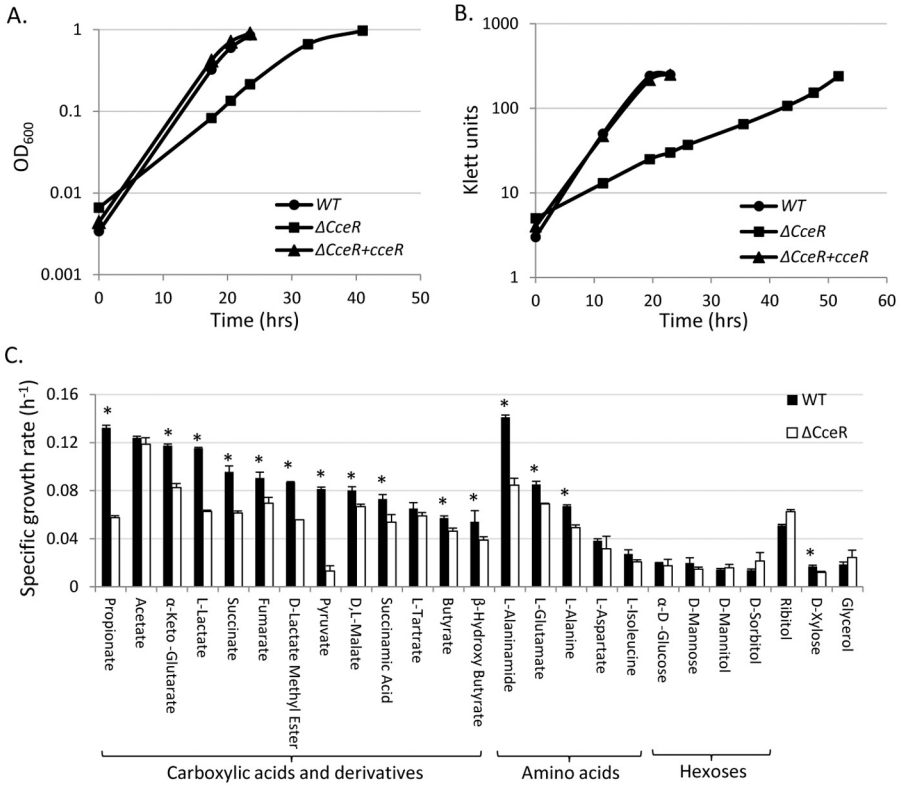

FIG 1 Growth phenotypes of the ΔCceR strain. Growth of WT, ΔCceR, and ΔCceR cells complemented with *cceR* from an IPTG-inducible plasmid (ΔCceR+*cceR*) on SMM under aerobic (A) and photosynthetic (B) conditions. Doubling times of WT, ΔCceR, and ΔCceR+*cceR* cells were 3.24 (3.22), 4.74 (10.35), and 2.95 (3.14) h, respectively, under aerobic (photosynthetic) conditions. (C) Specific growth rates of WT and ΔCceR strains on 25 individual carbon sources under aerobic respiratory conditions. Cells were grown in modified SMM in which succinate, glutamate, and aspartate were replaced with equimolar amounts of the carbon source under consideration (see Materials and Methods). Error bars represent standard errors from 3 independent replicates. *, carbon sources on which the WT specific growth rate was statistically significantly faster than that of the ΔCceR mutant.

which controls expression of photosynthesis-related genes in response to changes in the cellular redox state (32). In contrast, the differential expression of protein synthesis-related genes (those encoding tRNAs and ribosomal proteins) in the absence of CceR (see Dataset S1) likely reflects growth rate differences between the WT and ΔCceR strains under the growth conditions used for this analysis (Fig. 1A).

CceR binds to the promoters of central carbon metabolism genes. To test if any of these differentially expressed genes were direct targets for CceR, we assessed genome-wide DNA binding by this protein using chromatin immunoprecipitation followed by high-throughput sequencing (ChIP-seq) with a 3×Myc-tagged version of this TF. While the addition of epitope tags can affect protein stability and/or activity, we observed that the tagged CceR protein was able to complement the growth phenotype of a ΔCceR mutant, verifying its functionality (see Fig. S1A in the supplemental material). This analysis identified a total of 19 CceR binding sites across the genome (Table 1) that were mapped to the upstream regions of 16 operons (carrying a total of 32 genes). Consistent with the observations from the global gene expression analysis, CceR was bound upstream of genes encoding ED (*zwf*, *pgl*, *eda*) and glycolytic enzymes (*pgi* and *fbaB*), the ATP synthase operons (*atpHAGDC* and *atpIBEXF*), subunits of the TCA cycle succinate dehydrogenase complex (*sdhAB*), phosphoenolpyruvate carboxykinase (*pckA*), as well as the *cceR* promoter (Fig. 2B and Table 1). Of the 16 promoter regions bound by CceR, RNA levels from 5 of these operons or genes were significantly increased, while those from 2 were decreased in the presence of CceR (Table 1), supporting the hypothesis derived from the global gene expression assays (see above) that CceR functions both as an activator and a repressor of transcription. The operons predicted to be directly repressed by CceR coded for proteins in the ED pathway (Zwf, Pgl, and Eda) as well as Pgi. Other CceR target genes encoding central metabolic enzymes were apparently directly activated by this TF, since their RNA levels were reduced in the ΔCceR mutant. In addition to these known metabolic genes, CceR was bound upstream of genes (RSP_6037, RSP_6082, and RSP_7376) encoding proteins of unknown functions, which could indicate these proteins might have previously uncharacterized roles in carbon or energy metabolism.

CceR was also bound upstream of the *rpoH1* (encoding the σ-factor that mediates the heat shock response in *R. sphaeroides* [33, 34]) and *flgM* (encoding the anti-sigma factor to *fliA* [35]) genes (Table 1 and Fig. 2B). This observation might suggest that CceR also has a role in chemotaxis and stress responses; however, neither of these genes was differentially expressed in a CceR-dependent manner in the global gene expression datasets. Thus, conditions under which these CceR binding sites might be functional, if any, remain unresolved.

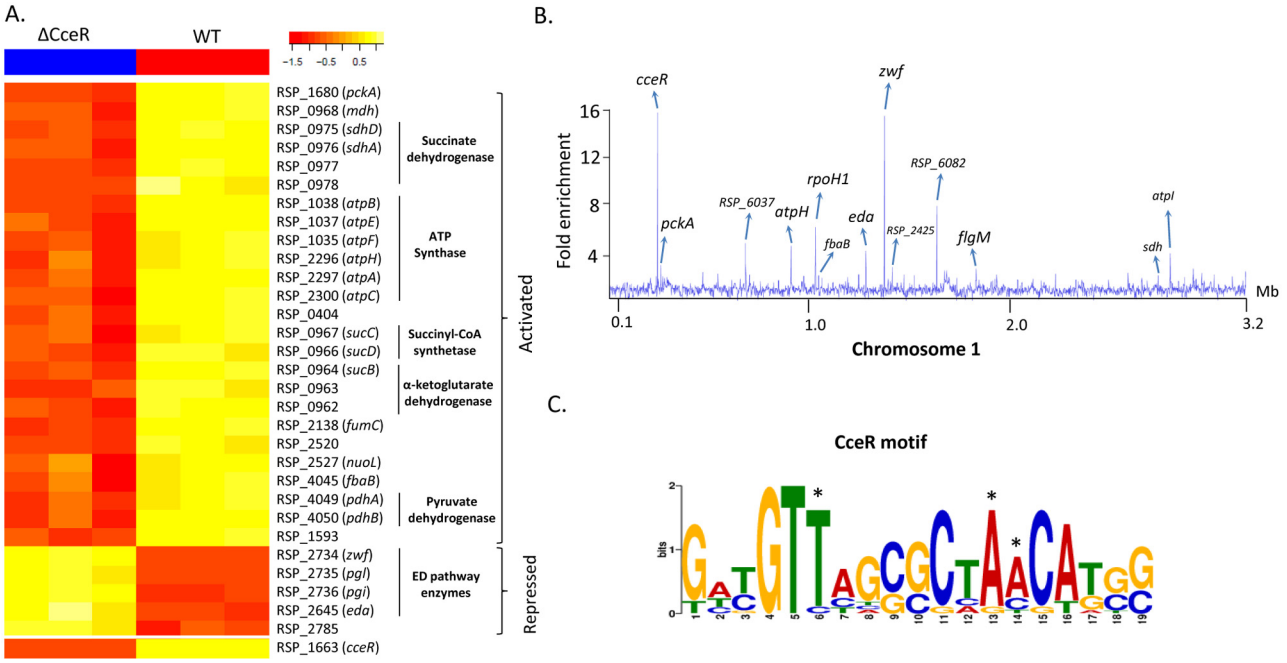

FIG 2 Genome-wide analysis of the role of CceR. (A) Heatmap highlighting differentially expressed metabolic genes between WT and ΔCceR cells under aerobic conditions. (B) Binding profile of CceR on *R. sphaeroides* chromosome 1. The gene names of only the first members of each operon are indicated. (C) Predicted CceR binding motif shared by sites identified in the ChIP-seq analysis. *, sites that were substituted in EMSA analysis.

Bases in the predicted consensus motif are required for CceR binding. Conducting *de novo* motif detection analysis on the sequences bound by CceR in ChIP-seq assays identified a shared inverted repeat sequence of (T/C)GTT N_6 AAC(A/T) (Fig. 2C) that is similar to the computationally predicted binding site for this TF (30). These ChIP-seq-predicted binding sites were located between 93 and 265 bp upstream of the start codon of the first gene in each predicted operon except in the case of the *zwf-pgl-pgi* operon (RSP_2734-6), where the predicted binding site was located 15 bp upstream. Given that the *zwf-pgl-pgi* operon is pre-

TABLE 1 CceR binding sites across the *R. sphaeroides* genome identified by ChIP-seq

No.	Gene ID	Annotation[a]	ChrID	ChIP FC[b]	Motif start	Predicted sequence[c]	Reg[d]
1	RSP_0037	*flgM*	chr1	2.4	1742534	GA**GGTT**CGGCCT**AACA**TGC	
2	RSP_0974-9	Succinate dehydrogenase complex (*sdh*)	chr1	1.7	2734837	CA**TGAT**TGCGCA**AACA**TGT	+
3	RSP_1039-35	F0F1 ATP synthase (*atpIBEXF*)	chr1	5.3	2801009	GA**TGTT**CGTGGT**GCAT**TCG	+
4	RSP_1663	*cceR*	chr1	18.7	255473	GC**CGTT**ATCGCT**AACA**TGG	ND
5	RSP_1680	Phosphoenolpyruvate carboxykinase (*pckA*)	chr1	5.4	272325	GA**CGTT**AGCGCA**ACCA**GCG	+
6	RSP_2296-2300	F0F1 ATP synthase (*atpHAGDC*)	chr1	7.3	918845	GA**TGTT**AGCGGC**ACCA**TCG	+
7	RSP_2410	RNA polymerase factor sigma-32 (*rpoH1*)	chr1	8	1039219	GA**CGTC**AGCGCT**ACCA**TGG	
8	RSP_2425	Putative CarD-like transcriptional regulator	chr1	2.4	1056109	GA**TTTT**CTAGCG**ACCA**TTC	
9	RSP_2646-5	*edd*, *eda*	chr1	6.7	1289714	TT**TGTT**AGCGCT**AACT**AGC	–
10	RSP_2734-6	*zwf*, *pgl*, *pgi*	chr1	16.9	1383134	GC**CGTT**AGCGCT**AACA**GGC	–
11	RSP_3896	*repC*	plasmidA	7.6	89831	GC**AGTT**TCTGCG**AACA**AGG	
12	RSP_3926	UDP-glucuronate 5′-epimerase	plasmidA	2.5	100456	CA**TGAT**AGCGCA**AACA**TCG	
13	RSP_4045	Fructose-bisphosphate aldolase (*fbaB*)	chr1	2.3	1127172	GT**TGTT**CGCGCT**AACT**TGG	+
14	RSP_6037	Hypothetical protein	chr1	7.1	692742	GC**TGTT**AGGGCA**AACA**TGG	NA
15	RSP_6082	Hypothetical protein	chr1	8.6	1642463	GT**TGTT**AGCGCC**AACA**TTC	NA
16	RSP_7376	Hypothetical protein	plasmidC	2.9	52671	GA**TGTT**CCGCCT**AACA**GCG	NA
17			chr2	2.6	704863	GA**GGTC**CGTGGC**AACA**TGG	NA
18			plasmidD	3.9	30048	TA**CGTT**TAGCCT**AACA**GCG	NA
19			plasmidC	2.7	54188	GT**TGTT**AGCCCT**GAGA**TCC	NA

[a] Binding sites not found ≤500 bp upstream of the start codon of an annotated gene were not assigned to any operon. Operons designated based on predicted operon structures (65).

[b] ChIP FC, ChIP-seq fold change (the fold enrichment of the CceR binding at target promoters relative to the mock anti-Myc ChIP control).

[c] Bold letters indicate the most conserved bases in the proposed CceR binding site.

[d] Regulatory role of CceR on target operon based on gene expression analysis. +, activation; –, repression; ND, not determined (this applies only to *cceR*, as the comparison between WT and the ΔCceR strain does not allow assessment of differential expression of the deleted *cceR* gene); NA, not applicable (these genes are not represented on the *R. sphaeroides* Affymetrix gene chip, and thus their expression levels could not be determined). No entry indicates that the genes were not observed to be differentially expressed under the conditions tested.

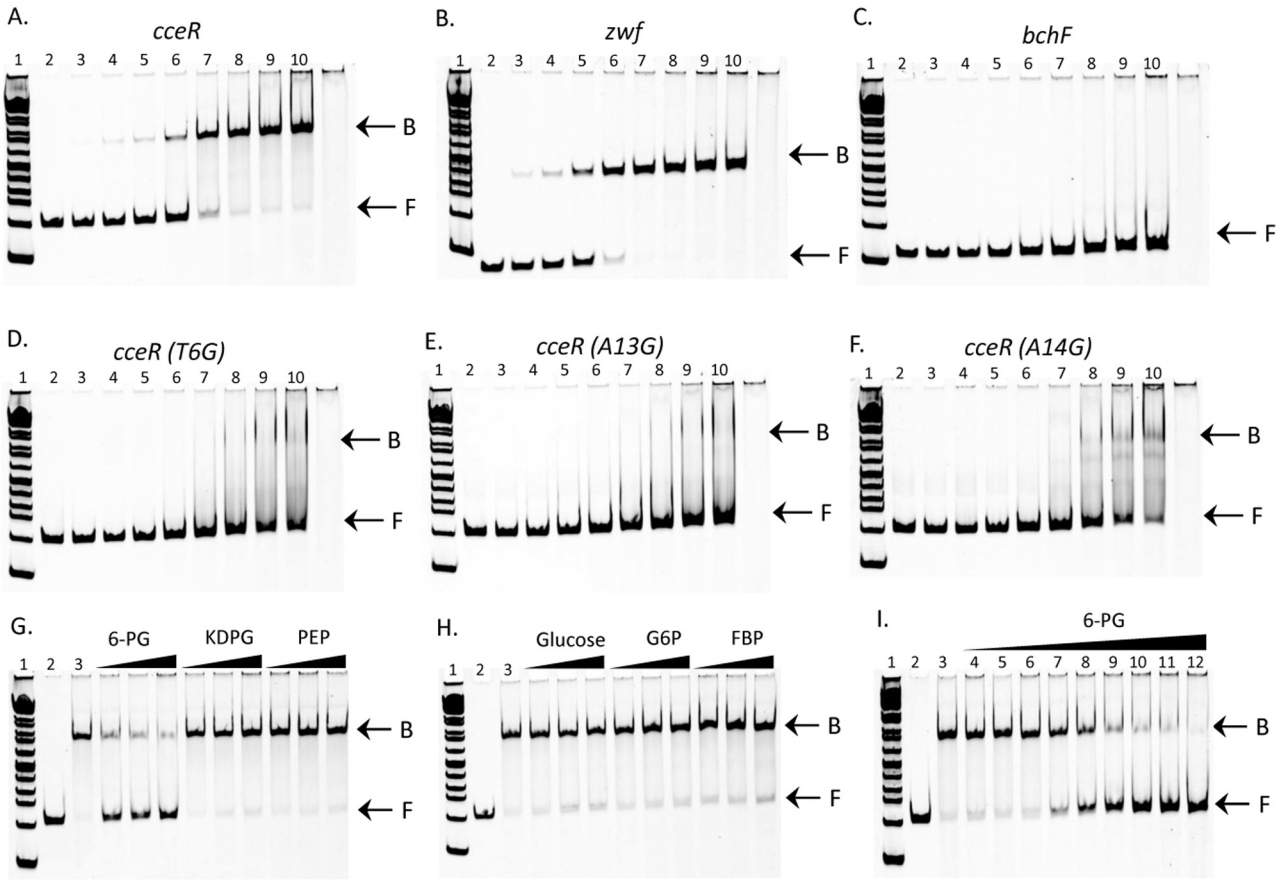

FIG 3 CceR binding specificity. Purified CceR was used for EMSA analysis with DNA fragments from the *cceR* (A), *zwf* (B), and *bchF* (C) promoters. Approximately 0.05, 0.1, or 0.085 μM of *cceR*, *zwf*, or *bchF* DNA fragment, respectively, was incubated with increasing amounts of CceR in each experiment. (D to F) EMSA analysis using templates with indicated point mutations, i.e., T6G, A13G, and A14G (or T92G, A85G, and A84G relative to the *cceR* start codon, respectively), in the predicted CceR binding site of the *cceR* promoter. For experiments in panels A to F, samples were loaded as follows: lane 1, 1-kb DNA ladder; lane 2, DNA only; lanes 3 to 10, DNA plus CceR (0.12, 0.24, 0.48, 0.97, 1.45, 1.94, 2.4, and 2.9 μM, respectively); lane 11, CceR only. B, bound DNA; F, free DNA. (G and H) Assessment of the effects of 6PG, KDPG, PEP, glucose, G6P, and FBP on CceR binding to DNA fragment from the *cceR* upstream regulatory region. Lane 1, 1-kb ladder; lane 2, DNA only; lane 3, DNA plus CceR. Three concentrations (0.5 mM, 2 mM, and 10 mM) were tested for each metabolite, with the increasing concentration gradient highlighted with the black triangle. Approximately 0.03 μM DNA and 1.94 μM CceR were used in each reaction. (I) Assessment of the effect of a range of 6PG concentrations on CceR binding activity. Samples were loaded as follows: lanes 1 to 3, 1-kb ladder, DNA only, and DNA plus CceR only, respectively; lanes 4 to 12, DNA, CceR, and 6-PG (0.01 μM, 0.1 μM, 1 μM, 10 μM, 50 μM, 100 μM, 0.5 mM, 2 mM, and 10 mM, respectively). Approximately 0.03 μM DNA and 1.94 μM CceR were used in each reaction.

dicted to be repressed by CceR, this may suggest that this TF acts in this case by blocking RNA polymerase binding or its clearance from this promoter (36).

To test if the predicted CceR binding motif contains sequence elements recognized by this TF, we analyzed its binding to target promoters using an electrophoretic mobility shift assay (EMSA). We found that purified CceR bound DNA fragments containing the predicted binding motif in the *R. sphaeroides cceR* and *zwf* promoters, with increasing concentrations of CceR protein resulting in increased amounts of bound DNA (Fig. 3A and B; see Fig. S2 in the supplemental material). If CceR binds DNA as a tetramer, as is the case for other LacI family members (37, 38), these data indicate that CceR binds the *zwf* promoter with an apparent affinity in the nanomolar range, similar to that observed for other TFs in this family (39). On the other hand, no detectable CceR binding was observed to a *bchF* promoter fragment (Fig. 3C), which was used as a control since it was not identified as a CceR target from the ChIP-seq data. Combined, these results predict that the CceR binding observed at the *cceR* and *zwf* promoters was due to sequence-specific protein-DNA interactions.

We made specific point mutations in the predicted CceR binding site of the *cceR* promoter to assess their impact on DNA binding. When we substituted the conserved thymidine at position 6 and adenines at positions 13 and 14 of the predicted CceR motif (Fig. 2C, corresponding to positions −92, −85, and −84, respectively, relative to the *cceR* start codon) with guanines, each of these single mutations had a detrimental effect on CceR binding (Fig. 3D to F). The T6G and A13G mutations resulted in a loss of CceR binding activity at all protein concentrations tested, indicating that these bases were critical for DNA recognition by CceR at the *cceR* promoter (Fig. 3D and E). The A14G mutation also resulted in a significant impairment of CceR binding. However, at higher protein concentrations, we observed CceR binding to this mutant DNA template (Fig. 3F), suggesting that CceR-DNA interactions are not completely nullified by the A14G mutation. The conservation of bases in the proposed consensus CceR motif

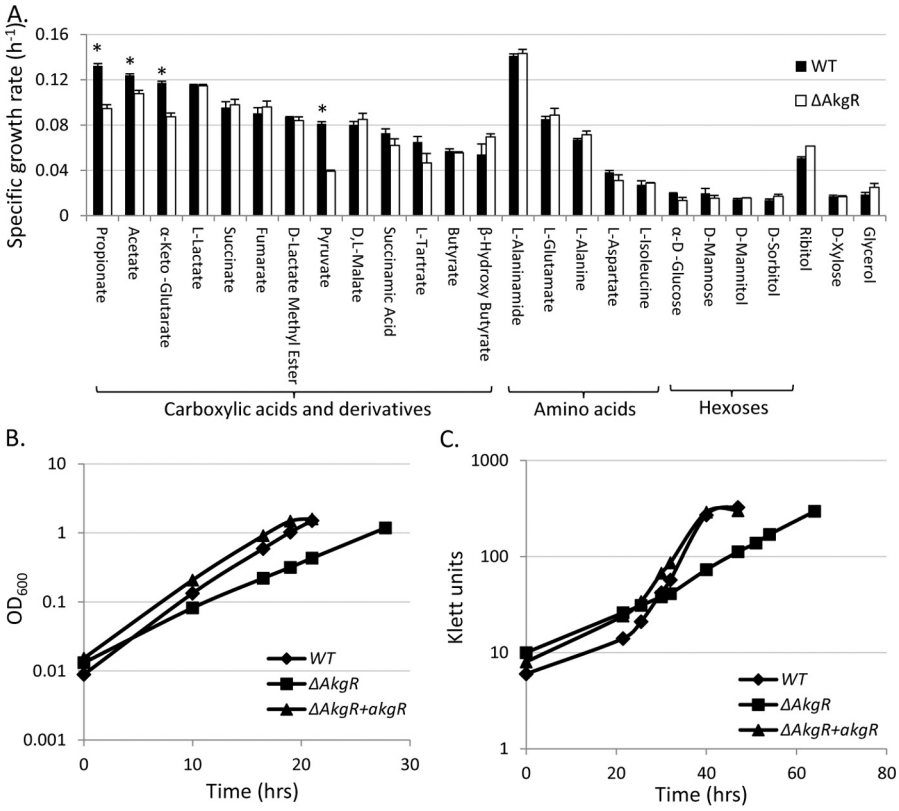

FIG 4 Growth of WT and ΔAkgR cells. (A) Specific growth rates of WT and ΔAkgR strains on 25 different carbon sources under aerobic conditions. Cells were grown in modified SMM in which succinate, glutamate, and aspartate were replaced with equimolar amounts of the carbon source under consideration (see Materials and Methods). Error bars represent standard errors from 3 independent replicates. *, carbon sources on which WT cells grew significantly faster than ΔAkgR cells. (B) Growth curves of WT, ΔAkgR, and ΔAkgR strains complemented with *akgR* from an IPTG-inducible plasmid (ΔAkgR+*akgR*) on α-ketoglutarate under aerobic conditions. The doubling times of WT, ΔAkgR, and ΔAkgR+*akgR* strains were 3.03, 4.61, and 3.04 h, respectively. (C) Growth curves of WT, ΔAkgR, and ΔAkgR+*akgR* strains on α-ketoglutarate under photosynthetic conditions. The doubling times of WT, ΔAkgR, and ΔAkgR+*akgR* strains were 4.5, 10.6, and 4.6 h, respectively.

(Fig. 2C) predicts that the A14 position has less information content than either T6 or A13, so the reduced impact on CceR binding of the A14G compared to the T6G or A13G mutations agrees with the properties of the predicted CceR binding site. In sum, these data indicate that the sequences predicted from *in vivo* studies are important for CceR DNA binding *in vitro*.

6-Phosphogluconate inhibits CceR DNA binding activity. LacI family TFs are generally composed of an N-terminal helix-turn-helix DNA binding domain and a C-terminal effector binding domain (EBD) (38). In well-studied members of this family, interactions between a ligand(s) and the EBD result in a conformational change of the TF, modulating its DNA binding activity (38). To test for ligands potentially recognized by the CceR EBD, we assayed the effects of central carbon metabolism intermediates 6-phosphogluconate (6PG), 2-keto-3-deoxy-6-phosphogluconate (KDPG), phosphoenolpyruvate (PEP), glucose, glucose-6-phosphate (G6P), and fructose-1,6-bisphosphate (FBP) on CceR binding to the *cceR* promoter fragment by EMSA (Fig. 3G and H). These assays showed that, of these metabolites, only 6PG significantly inhibits CceR DNA binding activity at the concentrations used (0.5 mM to 10 mM) (Fig. 3G). When we assessed the impact of lower concentrations of 6PG on CceR DNA binding, we found inhibitory effects at 6PG concentrations as low as 10 μM (Fig. 3I). These data indicate that 6PG has the ability to inhibit CceR DNA binding at physiologically relevant (micromolar) concentrations. Previous analysis indicated that the intracellular 6PG level is ~86 μM during growth with glucose as the main carbon source (40). When these data are considered in light of our *in vitro* DNA binding studies, it predicts that CceR activity is significantly reduced when the ED pathway is used for glucose metabolism. Given that glucose is metabolized almost exclusively via the ED pathway in *R. sphaeroides* (28, 29), the inhibition of CceR DNA binding by an ED pathway intermediate (i.e., 6PG) links activity of this TF to a pathway metabolite (see Discussion).

AkgR activates transcription of selected TCA cycle genes in *R. sphaeroides*. Another *R. sphaeroides* TF predicted to regulate transcription of genes encoding enzymes in central carbon and energy metabolism is the GntR family TF AkgR (30). To test the role of AkgR, we made an in-frame markerless deletion of *akgR* (ΔAkgR mutant) and compared the growth of this mutant to that of WT cells. The growth of ΔAkgR cells on succinate-containing SMM was equivalent to that of WT cells under both aerobic and anaerobic photosynthetic conditions (see Fig. S3), suggesting that any role of AkgR under these conditions is limited. However, when we assessed the growth of the ΔAkgR strain on SMM containing one of 25 carbon sources under aerobic conditions, we found that it exhibited a growth defect compared to WT cells on α-ketoglutarate, propionate, pyruvate, and acetate (Fig. 4A). Ad-

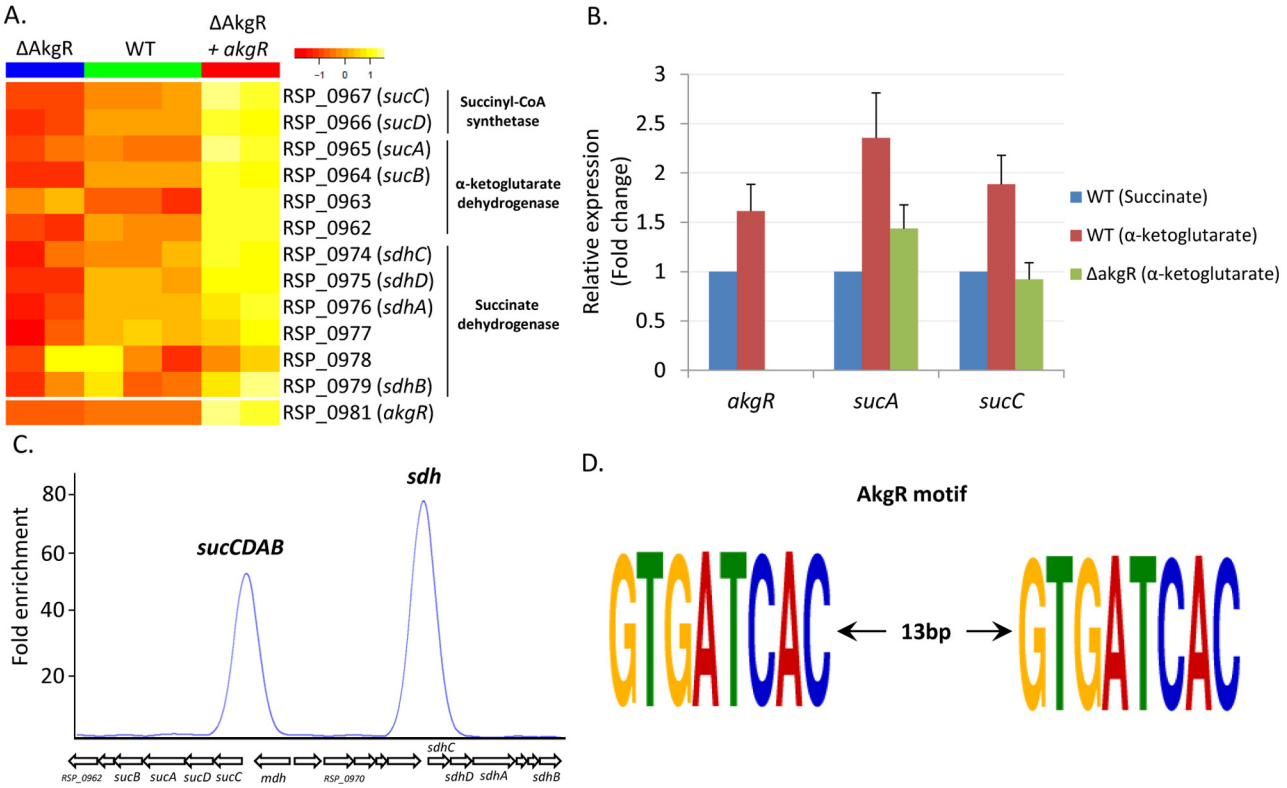

FIG 5 Genomic analysis of AkgR targets. (A) Heatmap highlighting differentially expressed metabolic genes between WT, ΔAkgR, and ΔAkgR+*akgR* strains during aerobic growth on SMM. (B) qRT-PCR analysis of the transcript levels of *akgR*, *sucC*, and *sucA* in WT and ΔAkgR cells during aerobic growth on succinate or α-ketoglutarate. Error bars represent standard errors of the mean from 2 independent biological and 2 independent technical replicates. (C) AkgR ChIP-seq binding profile at *sucCDAB* and succinate dehydrogenase (*sdh*) promoter regions. (D) Predicted AkgR binding motif shared by ChIP-seq-identified target sites.

ditional growth experiments with α-ketoglutarate as the sole carbon source showed that under aerobic conditions, ΔAkgR cells grew ~1.5 times slower than WT cells (Fig. 4B), while the photosynthetic doubling time of this mutant was ~2.5 times slower than its WT parent on this carbon source (Fig. 4C).

AkgR-dependent expression is induced by growth on α-ketoglutarate. To gain insight into the role of AkgR, we conducted global gene expression assays on WT and ΔAkgR cells grown aerobically in succinate containing SMM. The only differentially expressed metabolic genes (cutoff of 1.5 FC, $P < 0.01$) identified in this analysis were those encoding subunits of succinyl coenzyme A (succinyl-CoA) synthetase (*sucD*; RSP_0966) and α-ketoglutarate dehydrogenase (*sucB*; RSP_0964), each of which had ~1.8-fold-higher transcript levels in WT cells than in ΔAkgR cells (Fig. 5A). These modest changes in global transcript levels are consistent with the lack of a growth phenotype observed for ΔAkgR cells grown on SMM.

Ectopic expression of *akgR* from an isopropyl-β-D-thiogalactopyranoside (IPTG)-inducible plasmid revealed a 2- to 3-fold increase in the abundance of transcripts encoding the subunits of succinyl-CoA synthetase (*sucCD*; RSP_0967-6), subunits of the succinate dehydrogenase complex (RSP_0974-9), and those in the α-ketoglutarate dehydrogenase complex (*sucAB*; RSP_0965-2) in the AkgR ectopic expression strain (ΔAkgR+*akgR* strain) relative to the ΔAkgR strain (Fig. 5A). Combined, these data indicate that AkgR directly or indirectly controls transcription of genes encoding these 3 TCA cycle enzymes.

Given the observed growth defect of the ΔAkgR strain during growth with α-ketoglutarate (Fig. 4), we used qRT-PCR to assess the transcript levels of *akgR*, *sucA*, and *sucC* in WT and ΔAkgR cells during growth on SMM containing either succinate (as a control) or α-ketoglutarate as the sole carbon source (Fig. 5B). We found that transcript levels of *sucA* and *sucC* were ~2.5- and 2-fold higher, respectively, in WT cells grown on α-ketoglutarate than those grown on succinate. These observations are consistent with an increased need for succinyl-CoA synthetase (SucCD) and α-ketoglutarate dehydrogenase (SucAB) activity during growth on α-ketoglutarate. In addition, we observed an ~1.5-fold increase in the *akgR* RNA levels during growth of WT cells on α-ketoglutarate relative to growth on succinate, suggesting that AkgR may be involved in activating transcription of these TCA cycle genes. Consistent with this hypothesis, the *sucA* and *sucC* transcript levels were ~2-fold lower in ΔAkgR cells than in WT cells grown on α-ketoglutarate (Fig. 5B).

AkgR binds to the promoters of operons encoding TCA cycle enzymes. To test for genome-wide DNA binding of AkgR, we conducted ChIP-seq with a 3×Myc-tagged AkgR protein that complements the growth defect of the ΔAkgR strain (see Fig. S1B in the supplemental material). The 9 genomic regions enriched for AkgR binding (Table 2) included those upstream of the succinyl-CoA synthetase and α-ketoglutarate dehydrogenase complex operon (*sucCDAB*; RSP_0967-2) and the succinate dehydrogenase complex operon (*sdh*; RSP_0967-2) (Fig. 5C). In addition, 7 other genomic regions were enriched for AkgR binding, but the physiological importance of these interactions is unknown, as no

TABLE 2 AkgR and other binding sites across the *R. sphaeroides* genome identified by ChIP-seq

Binding site	No.	Gene ID	Annotation[a]	ChrID	ChIP FC[b]	Motif start	Predicted sequence[c]	Reg[d]
AkgR targets	1	RSP_0967-2	sucCDAB	chr1	57.8	2730051	**GTGATCAC**GGGCTCGAAGGGT**GTGATCAC**	+
	2	RSP_0974-9	Succinate dehydrogenase complex (*sdh*)	chr1	84.4	2734855	**GTGATCAC**AGGCCCGCATCTT**GTGATCAC**	+
Other	3	RSP_1718	50S ribosomal protein L23	chr1	6.7	309349		
	4	RSP_3523	ABC peptide transporter	chr2	3.8	603190	**GTGATCAC**	
	5	RSP_2434	Putative MCP methyltransferase CheR1	chr1	4	1067862	**GTGATCAC**	
	6	RSP_0386	Cold-shock DNA-binding domain protein	chr1	2.8	2119408	**GTGATCAC**	
	7			chr1	7.8	950186	**GTTATCAC**	
	8			chr2	3.1	588319	**GTGATCAC**	
	9			chr1	2.9	3136550	**GTGATCAC**	

[a] Binding sites not found ≤500 bp upstream of the start codon of an annotated gene were not assigned to any operon.
[b] ChIP FC, ChIP-seq fold change (the fold enrichment of the CceR binding at target promoters relative to mock anti-myc ChIP control).
[c] Bold letters indicate the most conserved bases in the proposed AkgR binding site.
[d] Regulatory role of AkgR on target operon based on gene expression analysis. +, activation. No entry indicates that the genes were not observed to be differentially expressed under the conditions tested.

genes in the vicinity of these putative binding sites were differentially expressed in the global gene expression datasets (Table 2).

De novo motif detection analysis of sequences bound by AkgR *in vivo* identified the shared DNA sequence motif, GTGATCAC (Table 2). Interestingly, the upstream regulatory regions of the succinyl-CoA synthetase/α-ketoglutarate dehydrogenase complex and the succinate dehydrogenase complex operons possessed 2 copies of this GTGATCAC motif with a 13-bp spacer region (Fig. 5D). Given that these were the only 2 operons bound by AkgR *in vivo* that were also found to be differentially expressed in an AkgR-dependent manner in the global gene expression analyses, we propose that the functional motif recognized by AkgR at these operons is the inverted repeat sequence GTGATCAC N_{13} GTGATCAC. If this is true, then the 7 other binding locations identified in the genome-wide ChIP-seq analysis could represent nonfunctional AkgR half-sites, since they did not contain 2 copies of this GTGATCAC motif.

CceR and AkgR jointly regulate carbon and energy metabolism. Our data predict that both CceR and AkgR regulate central carbon and energy metabolism pathways in *R. sphaeroides*. While CceR has a larger predicted regulon and broader physiological impact than AkgR, their direct target genes overlap, as both TFs directly regulate expression of subunits of the succinate dehydrogenase complex. When growing on carbon sources that require significant TCA cycle activity (such as α-ketoglutarate and pyruvate), growth is impaired in both the ΔAkgR and ΔCceR single mutants (Fig. 6A and B), consistent with their roles in regulating expression of genes encoding TCA cycle enzymes. Furthermore, a ΔCceR ΔAkgR double mutant shows a more severe growth defect when using either α-ketoglutarate or pyruvate as a major carbon source than each of the single mutants (Fig. 6), indicating that these 2 TFs jointly regulate the expression of TCA cycle enzymes. Thus, we conclude that CceR and AkgR function cooperatively to regulate the expression of enzymes needed for the metabolism of substrates that require high flux through the TCA cycle.

DISCUSSION

This work provides significant new information on the networks that directly control transcription of central carbon and energy metabolism genes. We show that two previously uncharacterized TFs, CceR and AkgR, are direct transcriptional regulators of a significant portion of the central carbon and energy metabolism pathways in *R. sphaeroides* (Fig. 7). Below, we summarize the new insights our studies have provided on the transcriptional control of central carbon and energy metabolism in this and potentially other alphaproteobacteria. We also put our findings in the context of published information on the transcriptional control of central carbon and energy metabolism in other systems.

CceR is a previously uncharacterized regulator of central carbon and energy metabolism. Previous studies in *B. subtilis*,

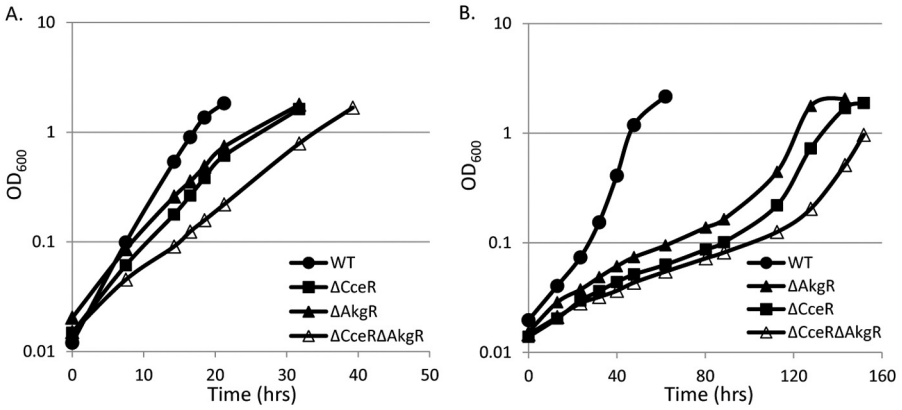

FIG 6 Growth of the ΔCceR ΔAkgR double deletion mutant on pyruvate and α-ketoglutarate. A comparison of the growth of WT, ΔCceR, ΔAkgR, and ΔCceR ΔAkgR strains with α-ketoglutarate (A) or pyruvate (B) as the main carbon source under aerobic conditions.

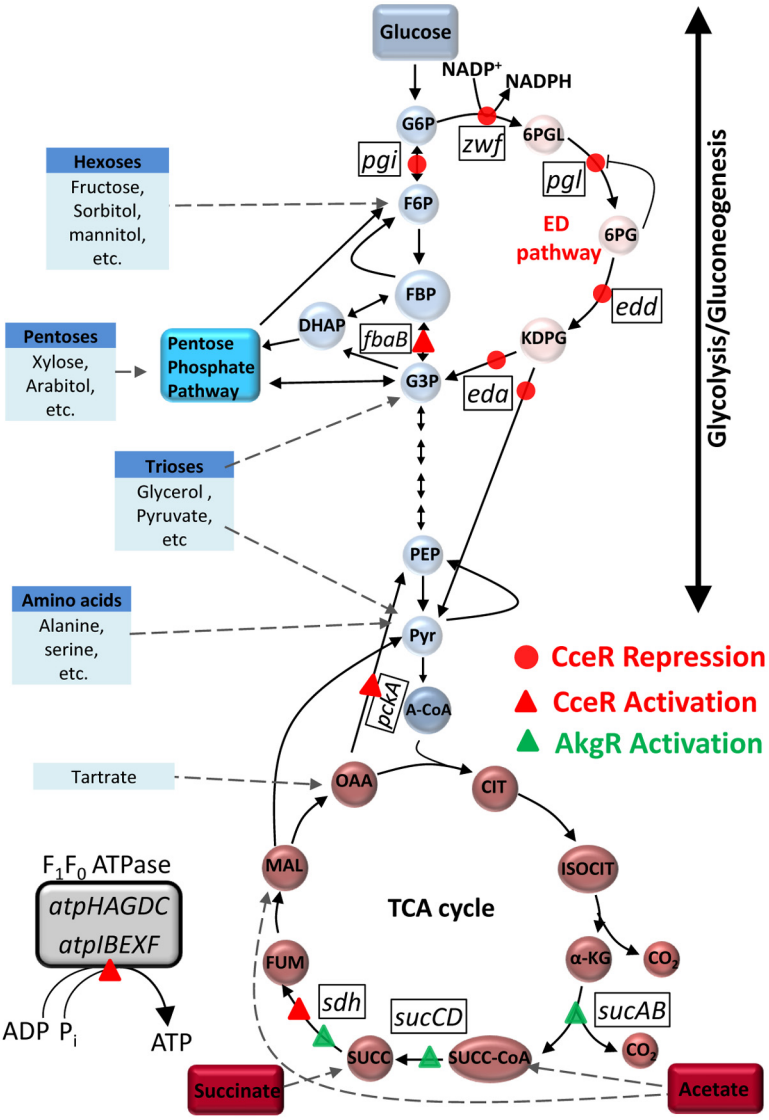

FIG 7 Map of central carbon metabolism highlighting CceR and AkgR targets. Metabolic map highlighting genes regulated by CceR and AkgR in *R. sphaeroides* and the entry points of various carbon sources into central metabolism. The figure is adapted from Fig. 4 from reference 28. *pgi* (glucose-6-phosphate isomerase; RSP_2736), *zwf* (glucose-6-phosphate 1-dehydrogenase; RSP_2734), *pgl* (6-phosphogluconolactonase; RSP_2735), *edd* (6-phosphogluconate dehydratase; RSP_2646), *eda* (KDPG/KHG bifunctional aldolase; RSP_2645), *fbaB* (fructose-bisphosphate aldolase; RSP_4045), *pckA* (phosphoenolpyruvate carboxykinase; RSP_1680), *sucAB* (α-ketoglutarate dehydrogenase; RSP_0965-4), *sucCD* (succinyl-CoA synthetase; RSP_0967-6), *sdh* (succinate dehydrogenase; RSP_0974-9), *atpHAGDC* (F0F1 ATP synthase; RSP_2296-2300), *atpIBEXF* (F0F1 ATP synthase; RSP_1039-35). TCA, tricarboxylic acid; G6P, glucose 6-phosphate; F6P, fructose 6-phosphate; FBP, fructose 1,6-bisphosphate; G3P, glyceraldehyde 3-phosphate; DHAP, dihydroxyacetone phosphate; 6PGL, phosphoglucono-δ-lactone; 6PG, 6-phosphogluconate; KDPG, 2-keto-3-deoxy-6-phosphogluconate; PEP, phosphoenolpyruvate; Pyr, pyruvate; A-CoA, acetyl-CoA; CIT, citrate; ISOCIT, isocitrate; 2-OG, 2-oxoglutarate (α-ketoglutarate); SUCC-CoA, succinyl CoA; SUCC, succinate; FUM, fumarate; MAL, malate; OAA, oxaloacetate; PPP, pentose phosphate pathway.

E. coli, and *Pseudomonas putida* have identified CcpA (10), Cra (6), and HexR (12), respectively, as transcriptional regulators of genes encoding central carbon metabolism pathways (11, 41). In addition, the global regulator ArcA directly controls the expression of TCA cycle and respiratory enzymes in *E. coli* in response to oxygen availability (4, 42), while Crp mediates catabolite repression in *E. coli* (3). Transcriptional control of central carbon and energy metabolism in alphaproteobacteria had not previously been described, but it appeared that they might use different networks to control these processes since alphaproteobacterial genomes lack homologues of these well-studied TFs.

We found that the LacI family TF, CceR, is a direct transcriptional regulator of genes that encode enzymes of both central carbon and energy metabolism in *R. sphaeroides*. CceR is both an activator and repressor of transcription, and it is required for normal growth in the presence of different carbon sources both in the presence and absence of oxygen. The genes directly repressed by CceR encode proteins of the ED pathway, similar to genes that are repressed by Cra and HexR (6, 12). However, CceR directly activates transcription of at least one TCA cycle enzyme and the F_1F_0 ATP synthase operons in *R. sphaeroides*, which are not known or predicted targets for CcpA, Cra, or HexR. In addition, while Cra

and HexR each regulate transcription of genes encoding enzymes that function in the glyoxylate shunt in their respective hosts, this pathway is incomplete in *R. sphaeroides*, and the genes that encode predicted enzymes in this pathway are not directly regulated by CceR.

While the complement of genes regulated by CcpA, Cra, or HexR and the published phenotypes of deletion mutants of these TFs make them appear functionally analogous to CceR, there are important differences between CceR and these other TFs. For instance, the RpiR family TF HexR is often found in close proximity to glucose utilization operons in beta- and gammaproteobacteria (11). In contrast, Cra and CceR belong to the LacI family of TFs, and their structural genes are not located proximal to target genes. LacI homologues are a large class of TFs involved in regulating the utilization of specific carbon sources (38), but family members like Cra and CceR appear to have broader functions. In addition, a phylogenetic analysis of 159 LacI family TFs encoded in 22 alpha-, beta-, and gammaproteobacteria indicates that Cra and CceR belong to different clades or protein subfamilies (see Fig. S4 in the supplemental material). This analysis predicts that CceR is most closely related to *E. coli* gluconate metabolism regulatory proteins, GntR and IdnR, while an uncharacterized LacI family member (RSP_3700) is the most closely related *R. sphaeroides* protein to Cra. Consistent with the predicted evolutionary distance between Cra and CceR, the DNA sequence recognized by Cra (GCTGAANCGNTTCA) (8) is different from the CceR binding site we identified [(T/C)GTT N_6 AAC(A/T)] (Fig. 2C).

There are also differences in effector molecules recognized by CceR and Cra. Previous analyses have shown that frucoste-1-phosphate and FBP reduce DNA binding by Cra *in vitro* (43, 44). However, at the concentrations tested, FBP had no detectable effect on CceR DNA binding *in vitro* (Fig. 3H). Instead, we found that 6PG, at concentrations likely to be physiologically relevant, prevented DNA binding by CceR (Fig. 3G and I), indicating that the EBDs of CceR and Cra respond to different effector molecules. The individual ligands used by CceR and Cra to control DNA binding likely reflect differences in the preferred routes of glucose metabolism between *R. sphaeroides* and *E. coli*. In *E. coli*, glucose is metabolized primarily via the Embden-Meyerhof pathway, which uses frucoste-1-phosphate and FBP as intermediates (29). On the other hand, *R. sphaeroides* metabolizes glucose primarily via the ED pathway, in which 6PG is the product of the glucose 6-phosphate dehydrogenase reaction, the first committed step of the pathway (28, 29). Thus, the use of different effector molecules likely provides a way for CceR and Cra to control carbon metabolism in their respective hosts, with predicted changes in 6PG pools providing a way to relieve CceR repression of ED pathway structural genes when these enzymes are needed for glucose utilization (28, 29) (Fig. 7).

In *E. coli*, FBP functions as a global regulatory metabolite, since it acts as an allosteric effector for central carbon metabolic enzymes, such as pyruvate kinase and phosphoenolpyruvate carboxylase (45–47). Furthermore, since FBP also directly regulates the activity of Cra (43), it plays a central role, directly or indirectly, in the regulation of an array of metabolic enzymes. The intracellular levels of FBP rise during the use of glucose as a carbon source, and the signal of this increased glycolytic flux is conveyed by FBP to its target proteins (45). Similar global regulatory metabolites controlling central metabolism are yet to be identified in *R. sphaeroides* or other alphaproteobacteria. However, the preferential use of the ED pathway for glucose metabolism in *R. sphaeroides* suggested that FBP was unlikely to function as a signal for increased glycolytic flux in this organism. Our identification of 6PG as an effector for CceR (Fig. 7) suggests that it replaces FBP in *R. sphaeroides* as the signal for increased glycolytic flux, indirectly modulating the activities of several enzymes through its interaction with CceR. This observation also raises the intriguing possibility that 6PG could have a broader role in regulation of central metabolic enzymes in *R. sphaeroides*, beyond that achieved through CceR. Further experimental analysis is needed to assess the wider regulatory role, if any, of 6PG.

The accumulation of 6PG during increased glycolytic flux is predicted to reduce CceR-dependent activation of ATPase and succinate dehydrogenase. The resultant 6PG dependent change in CceR activity is also predicted to reduce formation of phosphoenolpyruvate and FBP from oxaloacetate and glyceraldehyde-3-phosphate, respectively (Fig. 7). Combined, our data suggest that CceR redirects metabolic flux through the central metabolism in response to 6PG availability, derepressing glycolysis and repressing gluconeogenesis when glucose (and thus 6PG) is abundant, while activating gluconeogenesis and repressing glycolysis during growth on alternative carbon sources (Fig. 7). Gluconeogenesis in concert with glucose-6-phosphate dehydrogenase (Zwf) activity has previously been shown to be an important alternative source of NADPH in *R. sphaeroides* in the absence of the pyridine nucleotide transhydrogenase during growth on carbon sources other than glucose (28). Thus, the activity of CceR can also have a major impact on the production of reduced pyridine nucleotides that are needed for growth, host microbe interactions, or the production of metabolic end products by this and other alphaproteobacteria.

Our data also predict that CceR activates the transcription of the *atp* operons in *R. sphaeroides* at low 6PG levels (Fig. 2A and Fig. 7). Conversely, the data also predict a relatively reduced expression of the ATPase operons during growth on glucose when 6PG levels are expected to be high. The 6PG levels observed during growth on glucose would prevent transcriptional activation of the ATPase operons by CceR. Since metabolism of glucose results in the generation of ATP by both substrate-level and oxidative phosphorylation, this predicted reduction in expression of the ATPase operon could reflect the use of transcriptional regulation to achieve a balance between ATP generation and energy consumption. Previously published analyses of the *E. coli* atp operon indicate that it is constitutively expressed (48). Thus, we propose that CceR provides a heretofore unrecognized transcriptional regulatory link between central carbon and energy metabolism in *R. sphaeroides* and possibly other bacteria.

CceR and AkgR are conserved among alphaproteobacterial species. Genes encoding homologues of CceR and AkgR are conserved in the genomes of other alphaproteobacteria. To assess the possible role of these CceR and AkgR homologues, we used the predicted CceR and AkgR binding sites to search for related DNA sequences across 20 representative alphaproteobacterial species covering the major subgroups of this class of bacteria. We found that CceR and AkgR binding sites are conserved among many *Rhodobacterales*, but CceR binding site are also found in several species of *Rhizobiales*, *Sphingomonadales*, and *Caulobacterales* (Fig. 8; see also Fig. S5 in the supplemental material), which are all metabolically versatile alphaproteobacteria that are abundant in freshwater and marine ecosystems (14).

Within the *Rhodobacterales*, we found that the CceR binding

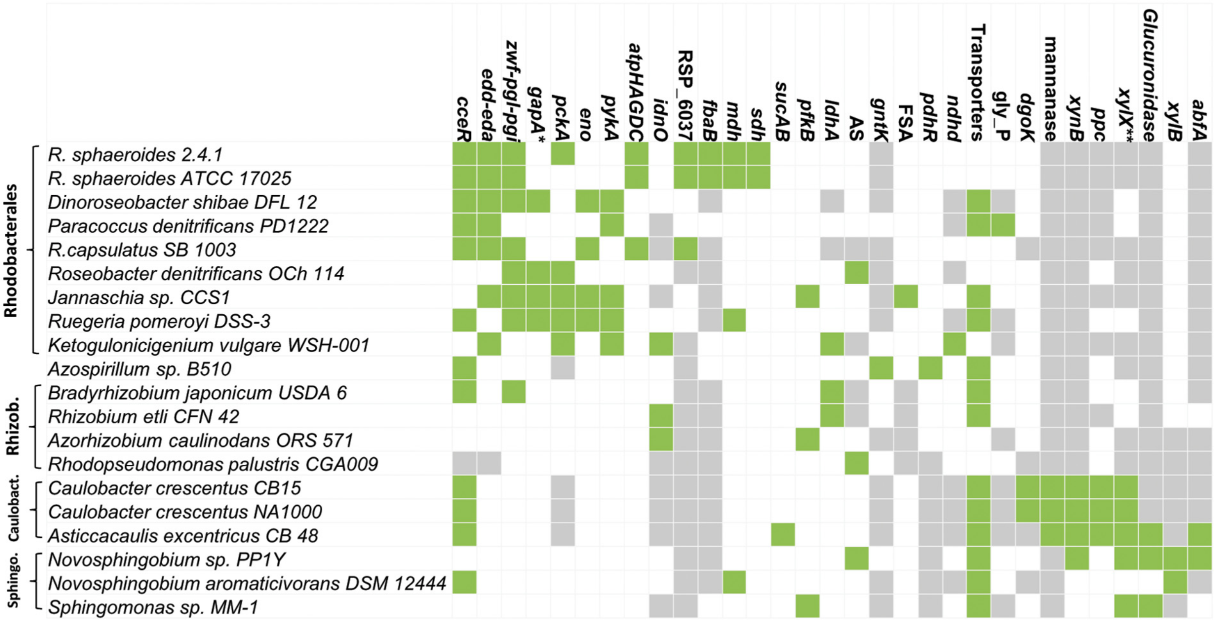

FIG 8 Conservation of CceR regulon across alphaproteobacteria. Predicted conservation of the CceR regulon across 20 alphaproteobacterial species based on the presence of a predicted CceR binding site upstream of the indicated genes. Green boxes indicate a candidate CceR binding site was located upstream of the gene, gray boxes indicate no ortholog for the specific protein was identified in that genome, while white boxes indicate the presence of orthologous protein but no candidate CceR binding site upstream of its encoding gene. CceR targets specific to *R. sphaeroides* 2.4.1 (i.e., *rpoH1*, *flgM*, *aptI*, RSP_2425, RSP_3896, RSP_3926, and RSP_7376) were omitted for brevity. Rhizob., *Rhizobiales*; Caulobact., *Caulobacterales*; Sphingo., *Sphingomonadales*; *edd*, 6-phosphogluconate dehydratase; *zwf*, glucose-6-phosphate 1-dehydrogenase; *pckA*, phosphoenolpyruvate carboxykinase; *atpHAGDC*, ATP synthase*gapA*-glyceraldehydes-3-phosphate dehydrogenase; *eno*, enolase; *pykA*, pyruvate kinase; *idnO*, gluconate 5-dehydrogenase; *fbaB*, fructose-bisphosphate aldolase; *mdh*, malate dehydrogenase; *sdh*, succinate dehydrogenase; *sucAB*, α-ketoglutarate dehydrogenase; *pfkB*, *pfkB* family carbohydrate kinase; *ldhA*, lactate dehydrogenase related; AS, acyl-CoA synthetase-like AMP binding protein; *gntK*, gluconokinase; FSA, fructose-6-phosphate aldolase; *pdhR*, pyruvate dehydrogenase regulator; *ndhd*, NADH dehydrogenase; transporter, ABC/TonB-dependent/TRAP family substrate transporters; gly_P, glycogen phosphorylase; *dgoK*, 2-dehydro-3-deoxygalactonokinase; *xynB*, xylan beta-1,4-xylosidase; *ppc*, phosphoenolpyruvate carboxylase; *xylX*, fumarylacetoacetate (FAA) hydrolase family protein *xylB*-xylulokinase; *abfA*, α-*n*-arabinofuranosidase. *, *gapA* includes both *gapA1* and *gapA2* in all species with predicted CceR binding sites upstream of these genes; **, the predicted CceR binding site for *xylX* in *C. crescentus* CB15 was identified ~91 bp downstream of the *xylX* start codon. In general, only intergenic regions were searched for potential CceR binding sites.

site was often located upstream of genes predicted to be involved in central carbon metabolism, suggesting that it serves a similar function in *R. sphaeroides* and these other species. We also found that the predicted CceR target genes vary in individual *Rhodobacterales* species encoding other enzymes in central carbon metabolism, such as glyceraldehyde-3-phosphate dehydrogenase (*gapA1* and *gapA2*), enolase (*eno*), pyruvate kinase (*pykA*), gluconate 5-dehydrogenase (*idnO*), glycogen phosphorylase, fructose-6-phosphate aldolase, and malate dehydrogenase (*mdh*), which were not identified as direct CceR targets in *R. sphaeroides* (Fig. 8). Within the *Sphingomonadales* and *Caulobacterales*, our comparative genomics analysis predicts that CceR may have evolved to regulate a different function. While CceR binding sites were found upstream of a few genes involved in central carbon metabolism, the vast majority of CceR sites were found upstream of genes predicted to be involved in the transport or metabolism of plant-derived carbon sources, such as mannans, xylans, and arabinoxylans, as well as sugars derived from them. In addition, our analysis also predicts that the role of the CceR homologue in the *Rhodospirillales* Azospirillum sp. B510 may be limited to lactate and pyruvate metabolism (by regulating the gene encoding the pyruvate dehydrogenase regulator, *pdhR*). These predicted differences in CceR target genes might reflect differences in the substrate utilization profiles of these diverse bacteria.

In addition to metabolic genes, putative CceR binding sites were also identified upstream of predicted transcriptional regulators in several organisms. For instance, we found CceR binding sites upstream of 3 TFs in *Dinoroseobacter shibae* (two LacI family and one LysR family TF) in addition to the one upstream of its *cceR* homologue. CceR binding sites upstream of TFs were also found in *R. sphaeroides* ATCC 17025, *Roseobacter denitrificans* Och 114, *Ruegeria pomeroyi* DSS-3, *Asticcacaulis excentricus* CB 48, and *Novosphingobium* sp. PP1Y. These observations suggest that CceR could have a broader (indirect) regulatory role in these species beyond that accounted for in its predicted regulon.

Our comparative genomic analyses also predicted that the proposed AkgR binding motif of GTGATCAC N_{13} GTGATCAC is typically located upstream of the *sucCDAB* and/or succinate dehydrogenase operons of *Rhodobacterales* (see Fig. S5 in the supplemental material), with only a few other putative members of an extended regulon, such as NADH dehydrogenase (*nuoA-N*), a tripartite tricarboxylate transporter (*tctA*), shikimate kinase, and quinoprotein ethanol dehydrogenase (*exaA2*), identified in some species (see Fig. S5). Thus, it appears that AkgR has a conserved role in regulating expression of TCA cycle genes both in *R. sphaeroides* and other alphaproteobacterial species.

Combinatorial regulation of central carbon and energy metabolism in alphaproteobacteria by a set of previously uncharacterized

acterized TFs. This work used a combination of biochemical, genetic, genomic, and physiological analyses to test and confirm the role of previously uncharacterized TFs, CceR and AkgR, in central carbon and energy metabolism. Our findings support the predictions of the recently generated large-scale *R. sphaeroides* TRN (30). However, this TRN predicts there are likely still other, as-yet-unidentified TFs that play important roles in regulation of central carbon metabolism in *R. sphaeroides* and related bacteria (30). For example, genes encoding other enzymes of the TCA cycle and electron transport chain (citrate synthase, isocitrate dehydrogenase, and NADH dehydrogenase), which are not members of either the CceR or AkgR regulons, share evolutionarily conserved DNA sequences in their upstream regulatory regions, suggesting a common mode of transcriptional regulation by as-yet-unidentified TFs in *R. sphaeroides* and possibly other organisms. Furthermore, genes encoding enzymes required for acetate utilization via the ethylmalonyl-CoA pathway in *R. sphaeroides* (49) are also predicted to be jointly regulated via as-yet-unknown TFs. Thus, the regulation of central carbon and energy metabolism in *R. sphaeroides* and possibly many other alphaproteobacteria likely involves the interplay of CceR, AkgR, and several other TFs, some of which are still to be discovered.

In sum, our findings represent an important advance in understanding the transcriptional control of central carbon and energy metabolism in alphaproteobacteria. This is a large group of abundant bacteria that play key roles in host-microbe interactions, have important metabolic activities that are often not found in many well-studied bacteria, or are of interest for engineering to produce compounds of utility to society. Our findings provide insight for future analysis of carbon and energy metabolism in *R. sphaeroides*, for identifying additional regulators of these pathways, and for testing predictions on the existence and function of analogous systems in controlling central carbon and energy metabolism in other alphaproteobacteria.

MATERIALS AND METHODS

Bacterial strains and growth conditions. *R. sphaeroides* 2.4.1 was used as the parental strain in this study. The individual and double ΔCceR and ΔAkgR mutants were constructed in this background. *E. coli* DH5α was used as a plasmid host, and *E. coli* S17-1 was used to conjugate DNA into *R. sphaeroides* (see Dataset S2 in the supplemental material). *R. sphaeroides* cultures were incubated at 30°C in Sistrom's minimal medium (SMM) (31) or in SMM lacking glutamate and aspartate and with succinate replaced with an alternative carbon source. The molar concentration of carbon atoms of the carbon source was kept constant at 135.5 mM, equivalent to that of succinate in SMM. Cells were grown photosynthetically in screw-cap tubes unless stated otherwise. The optical density of photosynthetic cultures was measured using a Klett-Summerson photometer and is expressed in Klett units (1 Klett unit equals ~10^7 cells/ml). When required, the medium was supplemented with 3 to 5 μM IPTG and 25 μg/ml kanamycin. *E. coli* cells were grown in Luria Bertani (LB) medium at 37°C, supplemented with 50 μg/ml kanamycin where needed.

Construction of mutants and expression plasmids. ΔCceR, ΔAkgR, and ΔCceR ΔAkgR strains were constructed as in-frame markerless deletions of almost the entire open reading frames, as previously described (28), and deletions were confirmed by PCR and sequencing with specific primers (see Dataset S2 in the supplemental material). Plasmid constructs for the ectopic expression of 3×Myc-tagged CceR (C-terminal tag) and AkgR (N-terminal tag) were made using sequence-specific primers (see Dataset S2) and conjugated into the relevant *R. sphaeroides* strains selecting for plasmid-encoded kanamycin resistance.

Protein purification. To purify CceR, a His-tagged protein was made by cloning *cceR* into pIND5 (50) by using specific primers (see Dataset S2) lacking the native stop codon, thus allowing inclusion of the pIND5-encoded C-terminal 6×His tag. The pIND5-*cceR*-6×His plasmid was transferred to *E. coli* BL21(DE3) (Novagen). Five milliliters of *E. coli* cells harboring pIND5-*cceR*-6×His were grown overnight in LB supplemented with 50 μg/ml kanamycin and then inoculated into 250 ml of fresh LB supplemented with 50 μg/ml kanamycin and 500 μM IPTG and incubated at 30°C for ~5 h until cells reached an optical density at 600 nm (OD_{600}) of ~0.6. One hundred milliliters of cells was harvested by centrifugation and lysed by sonication in buffer containing 50 mM NaH_2PO_4, 100 mM NaCl, 10 mM imidazole, 10% glycerol, and 0.25 m/ml lysozyme. The suspension was centrifuged and CceR-6×His was purified from the supernatant by Ni2+ affinity chromatography (Qiagen). The slurry was washed 3 times and then CceR-6×His was eluted in buffer containing 50 mM NaH_2PO_4, 300 mM NaCl, 250 mM imidazole, and 10% glycerol. Protein samples were stored in ~50% glycerol at −80°C until use. Protein was quantified using Lowry assay (51).

Electrophoretic mobility shift assay. To assess *in vitro* binding of CceR to target promoters, assays were conducted with the EMSA kit (E33075; Life Technologies). Target DNA fragments were amplified by PCR from genomic DNA using specific primers (see Dataset S2), and the DNA fragments were gel purified. Increasing amounts of purified CceR (final concentration of monomers ranging from ~0.12 to 2.9 μM) were incubated with ~0.05 μM of purified target DNA for 45 min at room temperature in 1× EMSA binding buffer in 10-μl reaction mixtures. Samples were run on a 6% polyacrylamide retardation gel with prechilled TBE running buffer at 200 V for 35 min at 4°C. Gels were stained with SYBR green DNA stain for 25 min with continuous shaking in the dark at room temperature, washed twice with distilled water, and visualized on the Omega Lum C imager (Aplegen, Inc.). To assess the impact of metabolites on CceR binding, 0.5, 2, and 10 mM 6-phosphogluconate (6PG), 2-keto-3-deoxy-6-phosphogluconate, phosphoenolpyruvate, glucose, glucose 6-phosphate, and fructose-1,6-bisphosphate were added to binding assays containing ~0.03 μM DNA and ~1.94 μM purified CceR. Lower concentrations ranging from 0.01 μM to 10 mM of 6PG were used to further assess the effect of 6PG on CceR binding.

To test the role of individual bases in the predicted CceR motif on DNA binding by this CceR, a 194-bp DNA fragment upstream of *cceR*, starting from the base before the *cceR* start codon, was amplified from genomic DNA by PCR using specific primers (see Dataset S2). Three point mutations at positions A-84G, A-85G, and T-92G relative to the *cceR* start codon were made in the predicted CceR binding site by overlap extension PCR. The WT and mutated DNA fragments were incubated with purified CceR, and EMSA analysis was conducted as described above.

RNA extraction, qRT-PCR, and microarray analyses. RNA extraction and microanalysis were conducted as previously described (26, 52). Briefly, RNA was isolated from exponential-phase *R. sphaeroides* cultures that were grown aerobically using a succinate-based medium in 500-ml Roux bottles bubbled with 69% N_2, 30% O_2, and 1% CO_2. RNA isolation, cDNA synthesis, labeling, and hybridization to *R. sphaeroides* GeneChip microarrays (Affymetrix, Santa Clara, CA) were performed as previously described (52). We used a succinate-based minimal medium, since it has been used for the majority of published transcriptional profiling and genome-wide experiments. Microarray datasets were normalized by robust multichip average (RMA) to the $\log_2$ scale with background adjustment and quantile normalization (53). Statistical analysis of normalized data to identify differentially expressed genes was done using the Limma package (54). Correction for multiple testing was done using Benjamini-Hochberg correction (55). All analyses were conducted in the R statistical programming environment (http://www.R-project.org). Reverse transcription-quantitative PCR (qRT-PCR) experiments were conducted in duplicates for each biological replicate using SYBR green JumpStart Taq ReadyMix (Sigma-Aldrich). Relative expression was determined via the $2^{-\Delta\Delta CT}$ method, with efficiency correction (56). The *R. sphaeroides*

rpoZ gene was used for normalization. Primers used in this analysis are provided in Dataset S2 in the supplemental material.

Chromatin immunoprecipitation analysis. Chromatin immunoprecipitation was conducted as previously described (23) using cells grown in succinate-based minimal medium with a few modifications. We used a succinate-based minimal medium for these studies, since it has been used for the majority of transcriptional profiling and other published genome-wide experiments. Briefly, *R. sphaeroides* cells (Δ*cceR* pIND5-*cceR*-3×Myc and Δ*akgR* pIND5-*akgR*-3×Myc) were grown aerobically in 500-ml cultures with bubbling, as described above. Cells were treated with 3 to 5 μM IPTG at inoculation (i.e., the lowest IPTG concentration required to restore normal aerobic growth with the tagged protein) and harvested at an OD_{600} of ~0.35. Δ*cceR* pIND5-*cceR*-3×Myc cells were also grown photosynthetically in 500-ml Roux bottles bubbled with 95% N_2 and 5% CO_2 and treated with IPTG. Chromatin immunoprecipitation was conducted (57) using polyclonal antibodies against the Myc epitope tag (ab9132; Abcam PLC). Immunoprecipitated DNA samples were PCR amplified, gel purified (size selection of ~200 bp), and sequenced at the UW Biotechnology Center sequencing facility, using the HiSeq 2500 sequencing system (Illumina, Inc.). The 50-bp sequence tags were mapped to the *R. sphaeroides* 2.4.1 genome (ftp://ftp.ncbi.nih.gov/genomes/Bacteria/Rhodobacter_sphaeroides_2_4_1_uid57653/) using SOAP version 2.21 (58), allowing a maximum of 2 mismatches and no gaps.

Peaks were identified using MOSAiCS (59) at a false discovery rate of 0.05. The MOSAiCS analysis was conducted as a two-sample analysis involving a pairwise comparison between with ChIP-seq data obtained from cells with Myc-tagged proteins (CceR or AkgR) and ChIP-seq data obtained from WT cells (with no Myc-tagged proteins) immunoprecipitated using anti-Myc antibodies (used as the control). Motifs were identified from sequences under the peak regions using MEME (60). Genomic locations with both a significant ChIP-seq peak and shared motifs were considered true binding sites.

Phylogenetic tree construction. To construct a phylogenetic tree for LacI family TFs, 159 known or predicted LacI proteins from 22 species (7 gamma-, 3 beta-, and 12 alphaproteobacteria) (see Fig. S5 in the supplemental material) were aligned using ClustalX (61), and a phylogenetic tree was constructed via the neighbor-joining phylogenetic method with the Protdist program of PHYLIP (62), using 100 bootstrap pseudoreplicates to construct the consensus tree. The resulting tree was visualized with display tools from the interactive tree of life (iTOL) website (63).

Identification of putative CceR and AkgR regulons across alphaproteobacteria. To determine the conservation of the CceR and AkgR regulons across alphaproteobacteria, we used position weight matrices (PWMs) built from verified *R. sphaeroides* CceR and AkgR targets to search all intergenic sequences from 20 representative alphaproteobacterial species: *R. sphaeroides* 2.4.1, *R. sphaeroides* ATCC 17025, *R. capsulatus* SB 1003, *Roseobacter denitrificans* Och 114, *Dinoroseobacter shibae* DFL 12, *Paracoccus denitrificans* PD1222, *Rhodopseudomonas palustris* CGA009, *Bradyrhizobium japonicum* USDA 6, *Caulobacter crescentus* NA1000, *Ruegeria pomeroyi*, *Jannaschia* sp. CCS1, *Asticcacaulis excentricus CB48*, *Azospirillum* sp. B510, *Rhizobium etli*, *Novosphingobium* sp. PP1Y, *Azorhizobium caulinodans*, *Novosphingobium aromaticivorans* DSM 12444, *Sphingomonas* sp. MM-1, *Ketogulonicigenium vulgare*, and *Caulobacter crescentus* CB15. Searches were carried out using MAST (60). Only PWM hits with a *P* value of $<10^{-6}$ were considered putative CceR/AkgR targets. Orthologous proteins across species were determined via orthoMCL analysis (64).

SUPPLEMENTAL MATERIAL

Supplemental material for this article may be found at http://mbio.asm.org/lookup/suppl/doi:10.1128/mBio.02461-14/-/DCSupplemental.

Figure S1, TIF file, 0.1 MB.
Figure S2, TIF file, 0.1 MB.
Figure S3, TIF file, 0.1 MB.
Figure S4, TIF file, 1 MB.
Figure S5, TIF file, 0.4 MB.
Dataset S1, XLSX file, 0.03 MB.
Dataset S2, XLSX file, 0.02 MB.

ACKNOWLEDGMENTS

This work was supported by the Department of Energy, Office of Science, Great Lakes Bioenergy Research Center (DE-FC02-07ER64494), the Genomics:GTL and SciDAC programs (DE-FG02-04ER25627), and a William H. Peterson Predoctoral Fellowship from the University of Wisconsin-Madison Bacteriology Department to S.I.

REFERENCES

1. **Hueck CJ, Hillen W.** 1995. Catabolite repression in *Bacillus subtilis*: a global regulatory mechanism for the Gram-positive bacteria? Mol Microbiol **15:**395–401. http://dx.doi.org/10.1111/j.1365-2958.1995.tb02252.x.
2. **Stülke J, Hillen W.** 1998. Coupling physiology and gene regulation in bacteria: the phosphotransferase sugar uptake system delivers the signals. Naturwissenschaften **85:**583–592. http://dx.doi.org/10.1007/s001140050555.
3. **Botsford JL, Harman JG.** 1992. Cyclic AMP in prokaryotes. Microbiol Rev **56:**100–122.
4. **Park DM, Akhtar MS, Ansari AZ, Landick R, Kiley PJ.** 2013. The bacterial response regulator ArcA uses a diverse binding site architecture to regulate carbon oxidation globally. PLoS Genet **9:**e1003839. http://dx.doi.org/10.1371/journal.pgen.1003839.
5. **Cunningham L, Georgellis D, Green J, Guest JR.** 1998. Co-regulation of lipoamide dehydrogenase and 2-oxoglutarate dehydrogenase synthesis in *Escherichia coli*: characterisation of an ArcA binding site in the *lpd* promoter. FEMS Microbiol Lett **169:**403–408. http://dx.doi.org/10.1111/j.1574-6968.1998.tb13347.x.
6. **Saier MH, Jr, Ramseier TM.** 1996. The catabolite repressor/activator (Cra) protein of enteric bacteria. J Bacteriol **178:**3411–3417.
7. **Ramseier TM, Bledig S, Michotey V, Feghali R, Saier MH, Jr.** 1995. The global regulatory protein FruR modulates the direction of carbon flow in *Escherichia coli*. Mol Microbiol **16:**1157–1169. http://dx.doi.org/10.1111/j.1365-2958.1995.tb02339.x.
8. **Shimada T, Yamamoto K, Ishihama A.** 2011. Novel members of the Cra regulon involved in carbon metabolism in *Escherichia coli*. J Bacteriol **193:**649–659. http://dx.doi.org/10.1128/JB.01214-10.
9. **Moreno MS, Schneider BL, Maile RR, Weyler W, Saier MH, Jr.** 2001. Catabolite repression mediated by the CcpA protein in *Bacillus subtilis*: novel modes of regulation revealed by whole-genome analyses. Mol Microbiol **39:**1366–1381. http://dx.doi.org/10.1046/j.1365-2958.2001.02328.x.
10. **Tobisch S, Zühlke D, Bernhardt J, Stülke J, Hecker M.** 1999. Role of CcpA in regulation of the central pathways of carbon catabolism in *Bacillus subtilis*. J Bacteriol **181:**6996–7004.
11. **Leyn SA, Li X, Zheng Q, Novichkov PS, Reed S, Romine MF, Fredrickson JK, Yang C, Osterman AL, Rodionov DA.** 2011. Control of proteobacterial central carbon metabolism by the HexR transcriptional regulator: a case study in *Shewanella oneidensis*. J Biol Chem **286:**35782–35794. http://dx.doi.org/10.1074/jbc.M111.267963.
12. **Del Castillo T, Duque E, Ramos JL.** 2008. A set of activators and repressors control peripheral glucose pathways in *Pseudomonas putida* to yield a common central intermediate. J Bacteriol **190:**2331–2339. http://dx.doi.org/10.1128/JB.01726-07.
13. **Daddaoua A, Krell T, Ramos JL.** 2009. Regulation of glucose metabolism in *Pseudomonas*: the phosphorylative branch and Entner-Doudoroff enzymes are regulated by a repressor containing a sugar isomerase domain. J Biol Chem **284:**21360–21368. http://dx.doi.org/10.1074/jbc.M109.014555.
14. **Garrity GM, Brenner DJ, Krieg NR, Staley JT, Krieg NR.** 2005. The proteobacteria: part C the α-, β-, δ-, and ε-proteobacteria. Springer, New York, NY.
15. **Gupta R, Mok A.** 2007. Phylogenomics and signature proteins for the alpha proteobacteria and its main groups. BMC Microbiol **7:**106. http://dx.doi.org/10.1186/1471-2180-7-106.
16. **Blankenship RE, Madigan MT, Bauer CE.** 1995. Anoxygenic photosynthetic bacteria. Advances in Photosynthesis and Respiration, Vol. 2 Springer, Netherlands.
17. **Hunter CN, Daldal F, Thurnauer MC, Beatty JT.** 2009. The purple phototrophic bacteria, vol **28**. Springer, New York, NY.
18. **Rutkis R, Kalnenieks U, Stalidzans E, Fell DA.** 2013. Kinetic modelling

of the Zymomonas mobilis Entner-Doudoroff pathway: insights into control and functionality. Microbiology **159:**2674–2689. http://dx.doi.org/10.1099/mic.0.071340-0.
19. **Skerker JM, Leon D, Price MN, Mar JS, Tarjan DR, Wetmore KM, Deutschbauer AM, Baumohl JK, Bauer S, Ibáñez AB, Mitchell VD, Wu CH, Hu P, Hazen T, Arkin AP.** 2013. Dissecting a complex chemical stress: chemogenomic profiling of plant hydrolysates. Mol Syst Biol **9:**674. http://dx.doi.org/10.1038/msb.2013.30.
20. **Franden MA, Pilath HM, Mohagheghi A, Pienkos PT, Zhang M.** 2013. Inhibition of growth of Zymomonas mobilis by model compounds found in lignocellulosic hydrolysates. Biotechnol Biofuels **6:**99. http://dx.doi.org/10.1186/1754-6834-6-99.
21. **Mackenzie C, Eraso JM, Choudhary M, Roh JH, Zeng X, Bruscella P, Puskás A, Kaplan S.** 2007. Postgenomic adventures with *Rhodobacter sphaeroides*. Annu Rev Microbiol **61:**283–307. http://dx.doi.org/10.1146/annurev.micro.61.080706.093402.
22. **Imam S, Yilmaz S, Sohmen U, Gorzalski AS, Reed JL, Noguera DR, Donohue TJ.** 2011. iRsp1095: a genome-scale reconstruction of the *Rhodobacter sphaeroides* metabolic network. BMC Syst Biol **5:**116. http://dx.doi.org/10.1186/1752-0509-5-116.
23. **Imam S, Noguera DR, Donohue TJ.** 2014. Global analysis of photosynthesis transcriptional regulatory networks. PLoS Genet. 2014. http://dx.doi.org/10.1371/journal.pgen.1004837.
24. **Zeilstra-Ryalls J, Gomelsky M, Eraso JM, Yeliseev A, O'Gara J, Kaplan S.** 1998. Control of photosystem formation in *Rhodobacter sphaeroides*. J Bacteriol **180:**2801–2809.
25. **Eraso JM, Kaplan S.** 1994. *prrA*, a putative response regulator involved in oxygen regulation of photosynthesis gene expression in *Rhodobacter sphaeroides*. J Bacteriol **176:**32–43.
26. **Dangel AW, Tabita FR.** 2009. Protein-protein interactions between CbbR and RegA (PrrA), transcriptional regulators of the *cbb* operons of *Rhodobacter sphaeroides*. Mol Microbiol **71:**717–729. http://dx.doi.org/10.1111/j.1365-2958.2008.06558.x.
27. **Joshi HM, Tabita FR.** 1996. A global two component signal transduction system that integrates the control of photosynthesis, carbon dioxide assimilation, and nitrogen fixation. Proc Natl Acad Sci U S A **93:**14515–14520. http://dx.doi.org/10.1073/pnas.93.25.14515.
28. **Imam S, Noguera DR, Donohue TJ.** 2013. Global insights into energetic and metabolic networks in *Rhodobacter sphaeroides*. BMC Syst Biol **7:**89. http://dx.doi.org/10.1186/1752-0509-7-89.
29. **Fuhrer T, Fischer E, Sauer U.** 2005. Experimental identification and quantification of glucose metabolism in seven bacterial species. J Bacteriol **187:**1581–1590. http://dx.doi.org/10.1128/JB.187.5.1581-1590.2005.
30. **Imam S, Noguera DR, Donohue TJ. 25 December** 2014. An integrated approach to reconstructing genome-scale transcriptional regulatory networks. PLoS Comput Biol. http://dx.doi.org/10.1371/journal.pcbi.1004103.
31. **Sistrom WR.** 1960. A requirement for sodium in the growth of *Rhodopseudomonas spheroides*. J Gen Microbiol **22:**778–785. http://dx.doi.org/10.1099/00221287-22-3-778.
32. **Swem LR, Gong X, Yu CA, Bauer CE.** 2006. Identification of a ubiquinone-binding site that affects autophosphorylation of the sensor kinase RegB. J Biol Chem **281:**6768–6775. http://dx.doi.org/10.1074/jbc.M509687200.
33. **Dufour YS, Imam S, Koo BM, Green HA, Donohue TJ.** 2012. Convergence of the transcriptional responses to heat shock and singlet oxygen stresses. PLOS Genet **8:**e1002929. http://dx.doi.org/10.1371/journal.pgen.1002929.
34. **Karls RK, Brooks J, Rossmeissl P, Luedke J, Donohue TJ.** 1998. Metabolic roles of a *Rhodobacter sphaeroides* member of the σ^{32} family. J Bacteriol **180:**10–19.
35. **Poggio S, Osorio A, Dreyfus G, Camarena L.** 2005. The flagellar hierarchy of *Rhodobacter sphaeroides* is controlled by the concerted action of two enhancer-binding proteins. Mol Microbiol **58:**969–983. http://dx.doi.org/10.1111/j.1365-2958.2005.04900.x.
36. **Rojo F.** 1999. Repression of transcription initiation in bacteria. J Bacteriol **181:**2987–2991.
37. **Lewis M, Chang G, Horton NC, Kercher MA, Pace HC, Schumacher MA, Brennan RG, Lu P.** 1996. Crystal structure of the lactose operon repressor and its complexes with DNA and inducer. Science **271:**1247–1254. http://dx.doi.org/10.1126/science.271.5253.1247.
38. **Weickert MJ, Adhya S.** 1992. A family of bacterial regulators homologous to Gal and Lac repressors. J Biol Chem **267:**15869–15874.
39. **Swint-Kruse L, Matthews KS.** 2009. Allostery in the LacI/GalR family: variations on a theme. Curr Opin Microbiol **12:**129–137. http://dx.doi.org/10.1016/j.mib.2009.01.009.
40. **Fuhrer T, Sauer U.** 2009. Different biochemical mechanisms ensure network-wide balancing of reducing equivalents in microbial metabolism. J Bacteriol **191:**2112–2121. http://dx.doi.org/10.1128/JB.01523-08.
41. **Antunes A, Camiade E, Monot M, Courtois E, Barbut F, Sernova NV, Rodionov DA, Martin-Verstraete I, Dupuy B.** 2012. Global transcriptional control by glucose and carbon regulator CcpA in *Clostridium difficile*. Nucleic Acids Res **40:**10701–10718. http://dx.doi.org/10.1093/nar/gks864.
42. **Donohue TJ, Kiley PJ.** 2010. Bacterial responses to O_2 limitation, p 17510701–189. In Storz G, Hengge R (ed), Bacterial stress responses, vol **2**. American Society for Microbiology, Washington, DC.
43. **Ramseier TM, Nègre D, Cortay JC, Scarabel M, Cozzone AJ, Saier MH, Jr.** 1993. *In vitro* binding of the pleiotropic transcriptional regulatory protein, FruR, to the *fru*, *pps*, *ace*, *pts* and *icd* operons of *Escherichia coli* and *Salmonella* Typhimurium. J Mol Biol **234:**28–44. http://dx.doi.org/10.1006/jmbi.1993.1561.
44. **Shimada T, Fujita N, Maeda M, Ishihama A.** 2005. Systematic search for the Cra-binding promoters using genomic SELEX system. Genes Cells **10:**907–918. http://dx.doi.org/10.1111/j.1365-2443.2005.00888.x.
45. **Chubukov V, Gerosa L, Kochanowski K, Sauer U.** 2014. Coordination of microbial metabolism. Nat Rev Microbiol **12:**327–340. http://dx.doi.org/10.1038/nrmicro3238.
46. **Waygood EB, Mort JS, Sanwal BD.** 1976. The control of pyruvate kinase of *Escherichia coli*. Binding of substrate and allosteric effectors to the enzyme activated by fructose 1,6-bisphosphate. Biochemistry **15:**277–282. http://dx.doi.org/10.1021/bi00647a006.
47. **Xu YF, Amador-Noguez D, Reaves ML, Feng XJ, Rabinowitz JD.** 2012. Ultrasensitive regulation of anapleurosis via allosteric activation of PEP carboxylase. Nat Chem Biol **8:**562–568. http://dx.doi.org/10.1038/nchembio.941.
48. **Kasimoglu E, Park SJ, Malek J, Tseng CP, Gunsalus RP.** 1996. Transcriptional regulation of the proton-translocating ATPase (*atpIBEFHAGDC*) operon of *Escherichia coli*: control by cell growth rate. J Bacteriol **178:**5563–5567.
49. **Erb TJ, Berg IA, Brecht V, Müller M, Fuchs G, Alber BE.** 2007. Synthesis of C5-dicarboxylic acids from C2-units involving crotonyl-CoA carboxylase/reductase: the ethylmalonyl-CoA pathway. Proc Natl Acad Sci U S A **104:**10631–10636. http://dx.doi.org/10.1073/pnas.0702791104.
50. **Ind AC, Porter SL, Brown MT, Byles ED, de Beyer JA, Godfrey SA, Armitage JP.** 2009. Inducible-expression plasmid for *Rhodobacter sphaeroides* and *Paracoccus denitrificans*. Appl Environ Microbiol **75:**6613–6615. http://dx.doi.org/10.1128/AEM.01587-09.
51. **Lowry OH, Rosebrough NJ, Farr AL, Randall RJ.** 1951. Protein measurement with the Folin phenol reagent. J Biol Chem **193:**265–275.
52. **Tavano CL, Podevels AM, Donohue TJ.** 2005. Identification of genes required for recycling reducing power during photosynthetic growth. J Bacteriol **187:**5249–5258. http://dx.doi.org/10.1128/JB.187.15.5249-5258.2005.
53. **Bolstad BM, Irizarry RA, Astrand M, Speed TP.** 2003. A comparison of normalization methods for high density oligonucleotide array data based on variance and bias. Bioinformatics **19:**185–193. http://dx.doi.org/10.1093/bioinformatics/19.2.185.
54. **Smyth G.** 2004. Applications in genetics and molecular biology 3. Berkeley Electronic Press, Berkeley, CA.
55. **Benjamini Y, Hochberg Y.** 1995. Controlling the false discovery rate—a practical and powerful approach to multiple testing. J R Stat Soc B Methodol **57:**289–300.
56. **Livak KJ, Schmittgen TD.** 2001. Analysis of relative gene expression data using real-time quantitative PCR and the 2(-Delta Delta C(T)) method. Methods **25:**402–408. http://dx.doi.org/10.1006/meth.2001.1262.
57. **Dufour YS, Landick R, Donohue TJ.** 2008. Organization and evolution of the biological response to singlet oxygen stress. J Mol Biol **383:**713–730. http://dx.doi.org/10.1016/j.jmb.2008.08.017.
58. **Li R, Yu C, Li Y, Lam TW, Yiu SM, Kristiansen K, Wang J.** 2009. SOAP2: an improved ultrafast tool for short read alignment. Bioinformatics **25:**1966–1967. http://dx.doi.org/10.1093/bioinformatics/btp336.
59. **Kuan PF, Chung D, Pan G, Thomson JA, Stewart R, Keleş S.** 2011. A statistical framework for the analysis of ChIP-seq data. J Am Stat Assoc **106:**891–903. http://dx.doi.org/10.1198/jasa.2011.ap09706.

60. **Bailey TL, Boden M, Buske FA, Frith M, Grant CE, Clementi L, Ren J, Li WW, Noble WS.** 2009. MEME SUITE: tools for motif discovery and searching. Nucleic Acids Res **37:**W202–W208. http://dx.doi.org/10.1093/nar/gkp335.
61. **Larkin MA, Blackshields G, Brown NP, Chenna R, McGettigan PA, McWilliam H, Valentin F, Wallace IM, Wilm A, Lopez R, Thompson JD, Gibson TJ, Higgins DG.** 2007. Clustal W and Clustal X version 2.0. Bioinformatics **23:**2947–2948. http://dx.doi.org/10.1093/bioinformatics/btm404.
62. **Felsenstein J.** 1989. PHYLIP—phylogeny interference package (version 3.2). Cladistics **5:**164–166.
63. **Letunic I, Bork P.** 2011. Interactive tree of life v2: online annotation and display of phylogenetic trees made easy. Nucleic Acids Res **39:** W475–W478. http://dx.doi.org/10.1093/nar/gkr201.
64. **Li L, Stoeckert CJ, Jr, Roos DS.** 2003. OrthoMCL: identification of ortholog groups for eukaryotic genomes. Genome Res **13:**2178–2189. http://dx.doi.org/10.1101/gr.1224503.
65. **Dehal PS, Joachimiak MP, Price MN, Bates JT, Baumohl JK, Chivian D, Friedland GD, Huang KH, Keller K, Novichkov PS, Dubchak IL, Alm EJ, Arkin AP.** 2010. MicrobesOnline: an integrated portal for comparative and functional genomics. Nucleic Acids Res **38:**D396–D400. http://dx.doi.org/10.1093/nar/gkp919.